AGU PUBLICATIONS

Geophysical Research Letters

RESEARCH LETTER
10.1002/2017GL073073

Special Section:
Early Results: Juno at Jupiter

Plasma waves in Jupiter's high-latitude regions: Observations from the Juno spacecraft

S. S. Tetrick[1], D. A. Gurnett[1], W. S. Kurth[1], M. Imai[1], G. B. Hospodarsky[1], S. J. Bolton[2], J. E. P. Connerney[3], S. M. Levin[4], and B. H. Mauk[5]

[1]Department of Physics & Astronomy, University of Iowa, Iowa City, Iowa, USA, [2]Southwest Research Institute, San Antonio, Texas, USA, [3]Goddard Space Flight Center, Greenbelt, Maryland, USA, [4]Jet Propulsion Laboratory, Pasadena, California, USA, [5]Applied Physics Laboratory, The Johns Hopkins University, Laurel, Maryland, USA

Key Points:
- A new broadband plasma wave emission between 50 Hz and 40 kHz was discovered from Juno Waves data in Jupiter's high-latitude polar regions
- The plasma waves are assumed to be propagating in the whistler mode below 40 kHz
- Significant correlation found between Waves data and an upgoing electron beam from JEDI, indicating that the beam is the source of the radiation

Correspondence to:
S. S. Tetrick,
sadie-tetrick@uiowa.edu

Citation:
Tetrick, S. S., D. A. Gurnett, W. S. Kurth, M. Imai, G. B. Hospodarsky, S. J. Bolton, J. E. P. Connerney, S. M. Levin, and B. H. Mauk (2017), Plasma waves in Jupiter's high-latitude regions: Observations from the Juno spacecraft, *Geophys. Res. Lett.*, *44*, 4447–4454, doi:10.1002/2017GL073073.

Received 13 FEB 2017
Accepted 14 MAR 2017
Accepted article online 20 MAR 2017
Published online 25 MAY 2017

Abstract The Juno Waves instrument detected a new broadband plasma wave emission (~50 Hz to 40 kHz) on 27 August 2016 as the spacecraft passed over the low-altitude polar regions of Jupiter. We investigated the characteristics of this emission and found similarities to whistler mode auroral hiss observed at Earth, including a funnel-shaped frequency-time feature. The electron cyclotron frequency is much higher than both the emission frequency and local plasma frequency, which is assumed to be ~20–40 kHz. The *E*/*cB* ratio was about three near the start of the event and then decreased to one for the rest of the period. A correlation of the electric field spectral density with the flux of an upgoing 20 to 800 keV electron beam was found, with a correlation coefficient of 0.59. We conclude that the emission is propagating in the whistler mode and is driven by the energetic upgoing electron beam.

1. Introduction

In this paper we investigate the characteristics of a new plasma wave emission observed by the Waves instrument on the Juno spacecraft during the first pass over the low-altitude polar regions of Jupiter's magnetosphere. The Waves instrument measures the electric and magnetic field components of radio and plasma waves within the frequency range of 50 Hz to 40 MHz for electric fields and 50 Hz to 20 kHz for magnetic fields. The frequency-time spectrogram of this emission is illustrated in Figure 1. We will describe the characteristics of the emission, establish its mode of propagation, and discuss the possible mechanisms by which it is generated. The paper is organized into the following topics: wave characteristics and mode of propagation, origin of the radiation, and a summary of the results.

2. Wave Characteristics and Mode of Propagation

The new plasma wave emission was first observed on 27 August 2016 (day 240) during a pass over the northern Jovian polar region. Frequency-time spectrograms of the electric and magnetic field spectral densities detected during this pass are shown in Figure 1. The white line represents the electron cyclotron frequency as determined from the Magnetometer instrument [*Connerney et al.*, 2017]. The emission begins at 07:30 UT and lasts until 12:12 UT and occurs over a wide range of Jupiter's polar cap, including the main auroral oval, as shown by the red line in Figure 2. The fact that the emission occurs in both the electric and magnetic fields shows that the plasma wave is an electromagnetic wave. The emission has a maximum detectable frequency ranging from about 20 to 40 kHz over the entire duration of the emission, increasing in frequency slightly near the end. It should be noted that there is no clear cutoff in frequency in either the electric or magnetic field, but rather a gradual decrease until the wave intensity is no longer detected. The maximum detectable frequency is higher for the electric field compared to the magnetic field due to the better sensitivity of the electric field antenna and the fact that the observed magnetic field decreases to the noise level at a lower frequency. A prominent curved time-dependent low-frequency cutoff is observed near the beginning of the emission, from 07:30 to 08:45 UT, and a less prominent but similar feature occurs near the end of the emission, from 12:00 to 12:12 UT. This shape is reminiscent of funnel-shaped whistler mode auroral hiss emissions observed at Earth over the auroral region [*Gurnett et al.*, 1983], but with half of the funnel facing left near the beginning of the emission, and the other half of the funnel facing right (but with less curvature) near the end of the emission. The funnel shape of auroral hiss is believed to be due to whistler mode propagation at wave normal angles near the resonance cone, which causes the

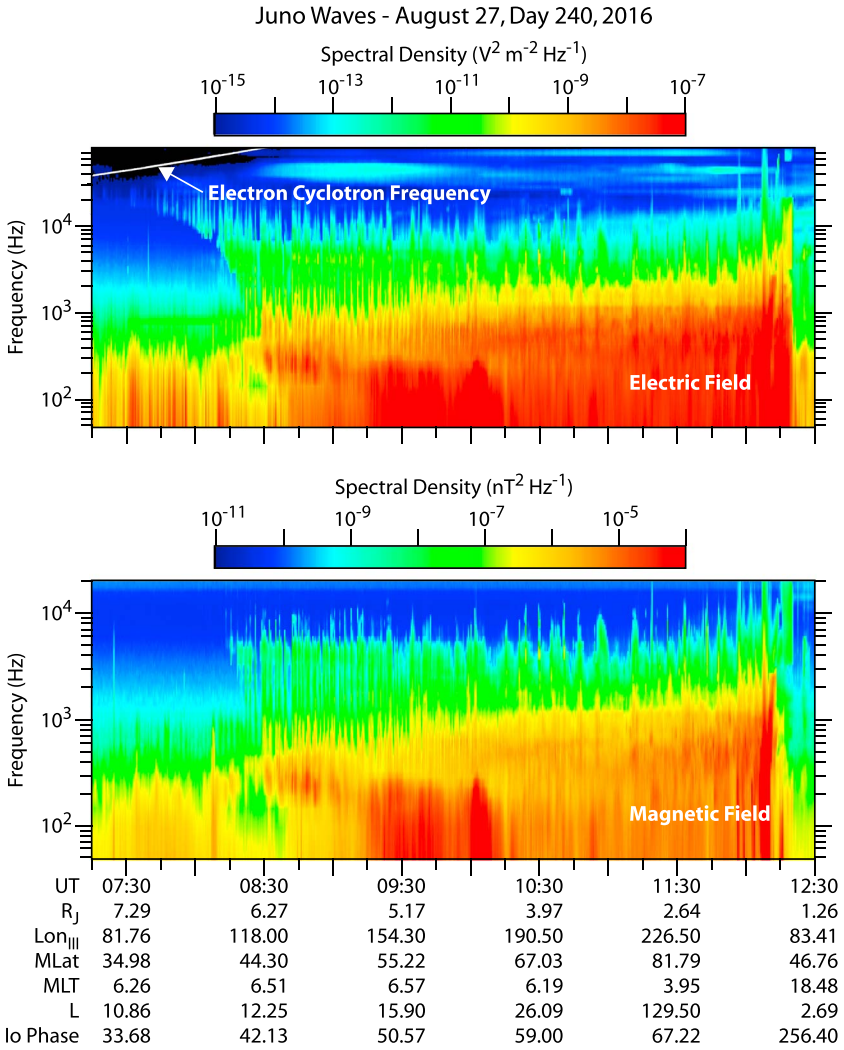

Figure 1. Frequency-time spectrograms of the electric and magnetic field spectral densities on day 240, corresponding to the first pass over the Jovian northern polar regions. The new plasma wave emission is observed between 07:30 and 12:12 UT in both the electric and magnetic field data. The emission at 12:15 UT is assumed to come primarily from electrostatic waves and not whistler mode emissions. The white line indicates the location of the electron cyclotron frequency, which is well above the observed emission frequency for the duration of the pass.

raypath to increasingly deviate from the magnetic field direction as the frequency increases [*Gurnett*, 1966; *Smith*, 1969; *Mosier and Gurnett*, 1969; *James*, 1976]. The resonance cone is defined as the region where the index of refraction goes to infinity in the cold plasma approximation [*Gurnett and Bhattacharjee*, 2005].

The relationship of the electric and magnetic field spectrums to the electron cyclotron frequency, ω_c, and electron plasma frequency, ω_p, provides vital clues for establishing the mode of propagation. First, we consider the electron cyclotron frequency, which begins at ~40 kHz at the start of the pass; see the white line in Figure 1, increasing to ~10 MHz near the end of the pass. The cyclotron frequency is then well above the frequency of the new plasma wave emission for the entire duration of the pass. The very large cyclotron frequency provides a highly different magnetospheric environment than is typical over Earth's polar region, where the cyclotron frequency is usually much closer to the frequencies of whistler mode auroral hiss emissions.

Next, we consider the relationship of the observed emission frequencies to the electron plasma frequency. Unfortunately, over the polar regions of Jupiter there is no clear indication in the Waves data of the local electron plasma frequency. Since the whistler mode can only propagate below either the electron

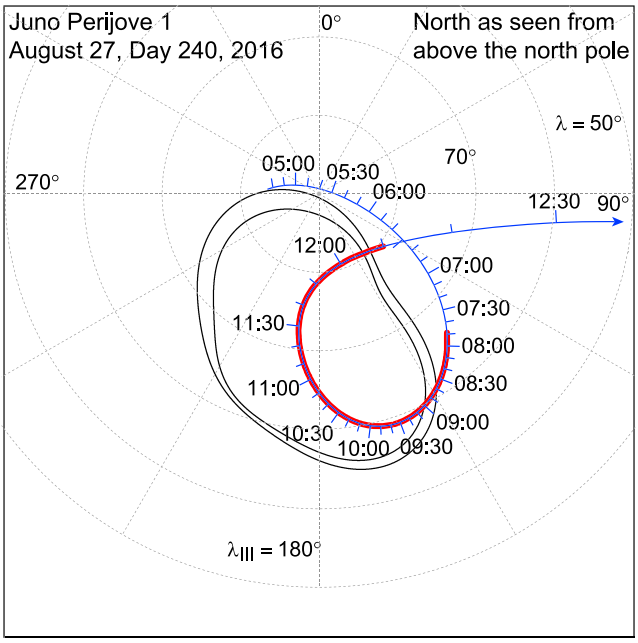

Figure 2. Plot of the trajectory of Juno (blue line) on 27 August, day 240, 2016. The magnetic projection onto Jupiter using the VIP4 magnetic field model [*Connerney et al.*, 1998] is shown. For the duration of the observed emission, the spacecraft passed over the statistical auroral oval based on Hubble UV observations (black ovals) and the northern polar cap region of Jupiter. The red line represents the interval during which the whistler mode emission was observed.

cyclotron frequency or the electron plasma frequency, whichever is lower, we have assumed that the plasma frequency is slightly above the maximum detectable frequency of the new emission, i.e., at about 20–40 kHz. We interpret the other narrowband emissions observed above about 40 kHz in the electric field spectrogram in Figure 1 as ordinary mode radio emissions, which would also be consistent with a plasma frequency near 20–40 kHz.

An important factor in identifying the mode of propagation is the electric to magnetic field ratio (E/cB), where c is the speed of light. Whistler mode emissions become quasi-electrostatic ($E \gg cB$) when the wave is propagating near the resonance cone, resulting in $E/cB > 1$ [see *Gurnett and Bhattacharjee*, 2005]. Figure 3 shows the observed color-coded (E/cB) ratios for the entire pass. As can be seen the (E/cB) ratio near the start of the left-facing half funnel-shaped emission (08:00–08:30 UT) is approximately three. An (E/cB) ratio significantly greater than one strongly supports the idea that the mode of propagation is the whistler mode. Although it should be noted that this value is not as high as sometimes occurs for whistler mode propagation near the resonance cone, the fact that the E/cB ratio is relatively modest is likely due to the emission not extending all the way up to the plasma frequency whereE/cB approaches infinity. After ~08:30 UT, the (E/cB) ratio decreases to about 1.0 to 1.5 for the rest of the pass, although around 09:30 UT near 1.5 kHz this ratio is approximately equal to 0.7. It should be noted that there is instrumental uncertainty in this ratio calculation due to the effective length of the electric field antenna.

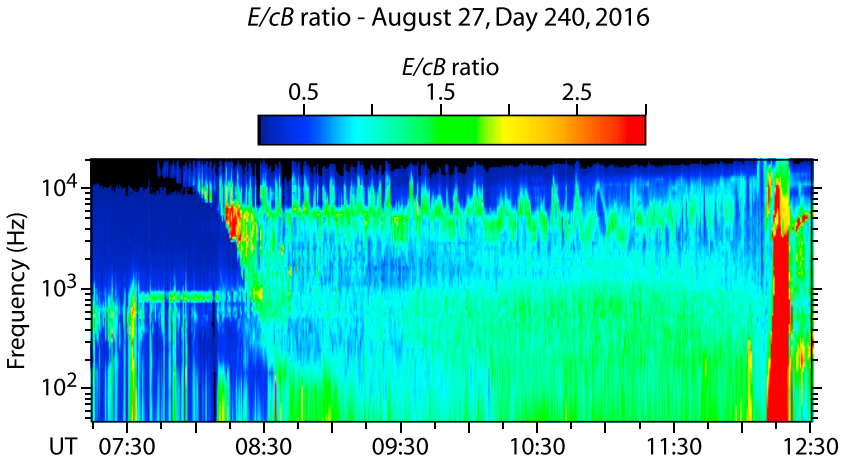

Figure 3. Frequency-time spectrogram of the E/cB ratio for day 240. The ratio is about three at the start of the pass, then decreases to one for the rest of the pass. The region with a large ratio around 12:15 is thought to be due primarily to electrostatic waves and not whistler mode emissions.

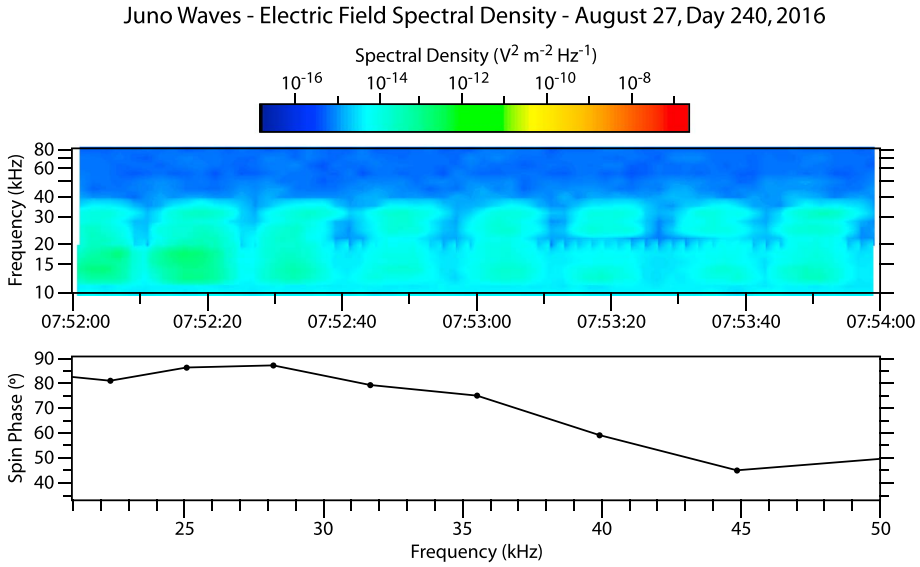

Figure 4. (top) The electric field spectral density near the start of the emission, depicting spin modulation in the electric field. (bottom) The spin phase of the maximum electric field relative to the planetary magnetic field, 0° representing $E \parallel B_0$, and 90° representing $E \perp B_0$. The frequency dependence in the spin phase can be seen. At lower frequencies $E \perp B_0$ and as frequency increases, the electric field becomes almost parallel to the planetary magnetic field.

That whistler mode *E*/*cB* ratios can be as small as one can be seen from the following equation which gives the index of refraction, $n \cong cB/E$, for parallel propagating, i.e., $\theta = 0$, right-hand polarized whistler mode waves [*Stix*, 1962]:

$$n^2 = 1 - \frac{\omega_p^2}{\omega(\omega - \omega_c)}$$

Note that when the cyclotron frequency becomes much larger than the plasma frequency, $\omega_c \gg \omega_p$, the second term after the equal sign becomes very small, much less than one. This causes the value for n to be nearly one, which means that $(E/cB) \approx 1$. Of course, at large wave normal angles, *E*/*cB* can become greater than one, eventually approaching infinity at the resonance cone.

Spin modulation measurements also provide another important tool for determining the mode of propagation. The Juno spacecraft is spin-stabilized and rotates in the right-hand sense around the axis of the spacecraft high gain antenna which is defined to be the +*z* axis. The spin period is 30 s. Because of the need to transmit data via the high gain antenna, the +*z* axis normally points toward Earth. The effective axis of the Waves electric antenna is oriented along the *y* axis, and the magnetic search coil antenna is oriented along the spacecraft *z* axis. In the interval where these measurements were made, it turns out that the +*z* axis was aligned approximately perpendicular to the Jovian magnetic meridian plane. This means that twice per rotation the electric antenna measures the component of the wave electric field parallel and perpendicular to the Jovian magnetic field. Figure 4 (top) shows an electric field spectrogram with a greatly expanded time scale near the edge of the left-facing funnel, from 07:52 to 07:54 UT. As can be seen, a strong spin modulation is apparent in the electric field spectral density, with alternating nulls and peaks at half the spin period. One can also see that the phase of the nulls and peaks increases with frequency. Figure 4 (bottom) shows the phase relative to the Jovian magnetic field (B_0), where a phase of 0° indicates $E \parallel B_0$ and a phase of 90° indicates $E \perp B_0$. As can be seen, the phase varies from about 90° at low frequencies to about 60° near ~40 kHz. This shows that the electric field is perpendicular to the Jovian magnetic field at low frequencies, tending toward parallel as the frequency increases.

This change in the direction of the electric field described above can be explained by the frequency dependence of the resonance cone angle, θ_{res}, which is the angle of the resonance cone relative to the magnetic field direction. The resonance cone angle is given by the following approximate equation:

$$\tan^2\theta_{\mathrm{res}} = -\frac{P}{S} = -\left(1-\frac{\omega_p^2}{\omega^2}\right)$$

where P and S are defined in *Stix* [1962] and we have used the approximation $\omega_c \gg \omega_p$ which implies $S \approx 1$. This equation explicitly shows that for whistler mode waves propagating near the resonance cone the electric field direction should vary from nearly perpendicular to the magnetic field at low frequencies to more nearly parallel to the magnetic field as the frequency increases, exactly as observed. This frequency-dependent feature of the spin modulation has been previously observed for whistler mode auroral hiss emissions at Earth and is illustrated in Figure 8 of *Gurnett et al.* [1983]. For the resonance cone angle given by the above equation to reliably give the electric field direction, the wave vector must be predominantly on one side of the resonance cone because otherwise it would average to a direction not easily related to the resonance angle. This wave vector distribution effect was previously shown via a multicomponent terrestrial study by *Santolik and Gurnett* [2002], in which a wide azimuthal distribution of wave vectors was found. For the spin modulation shown in Figure 4, the above condition is believed to be satisfied to a good approximation because the spacecraft at that time is located well equatorward of the magnetic field line on which the radiation is generated, which is believed to be first encountered at about 08:35 UT. Although terrestrial observations of auroral hiss [*Gurnett et al.*, 1983] typically show the electric field phase angle shifting to near 0° as the frequency approaches the plasma frequency, our measurements in Figure 4 only show a shift to about 50°. The reason why the phase shift does not extend to near 0° appears to be due to the fact that emission does not extend all the way up to the plasma frequency. Just what limits the upper frequency of the emission in this case is not known. One possibility is that it is caused by a shadow effect caused by a lower plasma frequency at some remote location along the raypath between the source and the spacecraft. Another possibility is that it is a source effect that somehow limits the maximum detectable frequency of the radiation.

3. Origin of the Radiation

Whistler mode plasma wave emissions can originate either from a remote source from elsewhere in the magnetosphere, or from a local source. A common locally generated source for whistler mode auroral hiss at Earth is an electron beam, which was first quantitatively studied by *Gurnett* [1966]. In order to see if the plasma wave emission is generated locally we compared the Waves data with particle measurements from the Jupiter Energetic-particle Detector Instrument (JEDI) [*Mauk et al.*, 2013]. An upward-going electron beam was detected by JEDI [*Mauk et al.*, 2017] over a similar time interval as the new emission observed by Waves. It should be noted that the energies of the upward-going electrons are a few orders of magnitude higher than those previously observed at Earth (typically hundreds of eV). However, at the outer planets, such as Saturn, electron energies associated with auroral hiss have been detected on the order of hundreds of keV [*Mitchell et al.*, 2005], consistent with the electron energies this study has observed. Figure 5 (first and second panels) show plots of the upward-going electron fluxes with pitch angles from 0 to 15° (energies of ~25 to $>$800 keV) from JEDI and the Waves electric field spectral density data (frequency range of 10^3 to 10^4 Hz). Upon initial visual analysis the electron beam and the electric field data seem to have similar upward-going trends and corresponding peaks and valleys. To test whether the whistler mode emission is generated by the electron beam, we performed a cross correlation. The electron fluxes were plotted against the integrated electric field strength, shown as a scatterplot in Figure 5 (third panel). This plot shows a clear upward linear trend. In order to determine the significance of the visual linear correlation, we computed a correlation coefficient (with 1 indicating a perfect correlation) and found it to be 0.59, indicative of a significant correlation. The significance of this correlation has been calculated based on the probability that a random distribution with N pairs of data points would produce a value of 0.59 for a coefficient. This probability (using $N = 210$) was found to be less than 0.00001; therefore, we consider our calculated correlation coefficient to be significant. This correlation provides evidence that the emission is in fact due to an electron beam, and we therefore assume that it is generated locally.

Experimental studies have shown clear evidence that electron beams can generate whistler mode auroral hiss emissions. In a 1986 study, done on the Spacelab 2 mission, an artificial electron beam was ejected from an electron gun on board a space shuttle and was detected by the Plasma Diagnostic spacecraft, supporting the idea of an electron beam being the source of the whistler mode auroral hiss emissions observed near Earth [*Gurnett et al.*, 1986]. Two proposed theories for the local generation of whistler mode emissions are

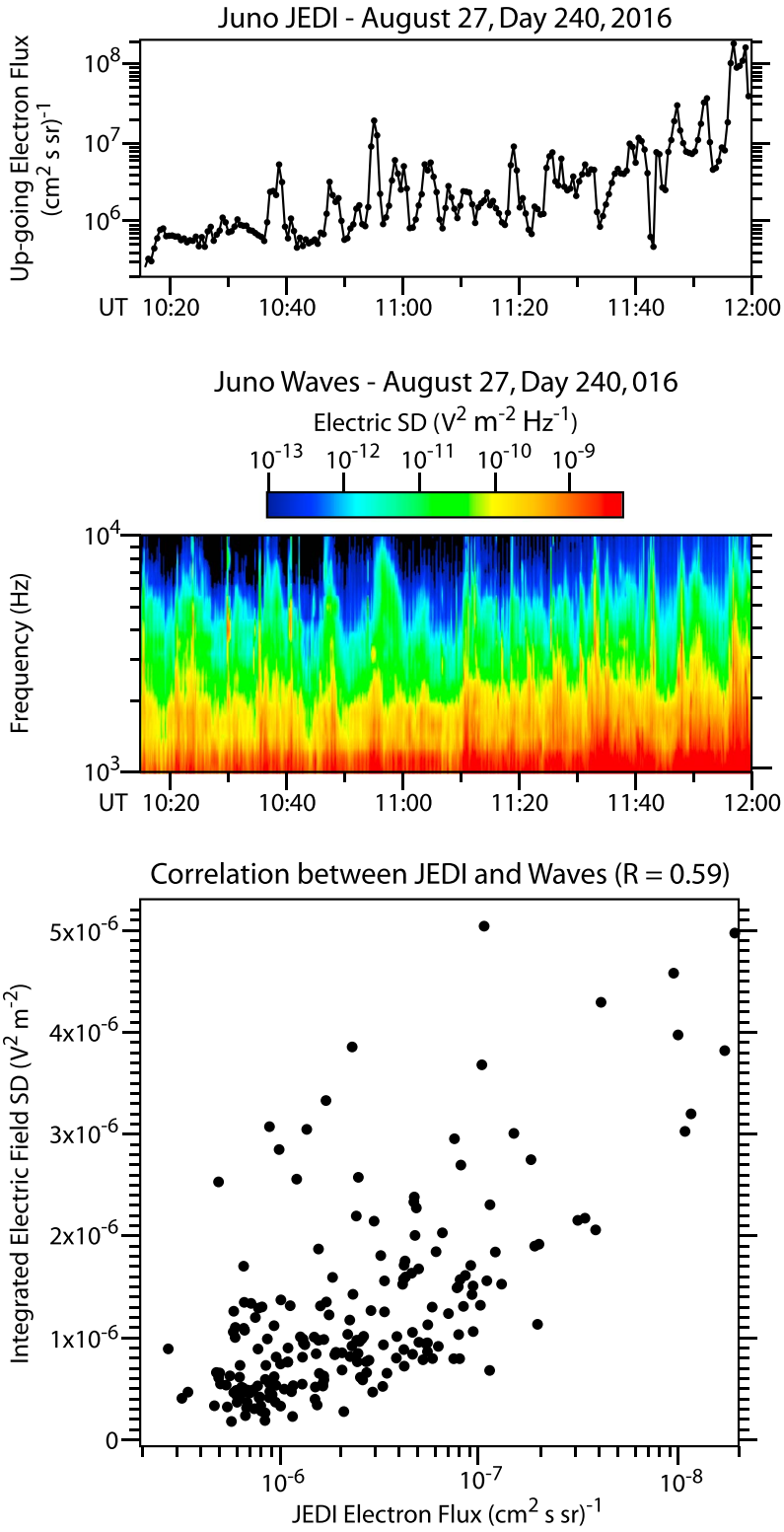

Figure 5. (first panel) The upgoing JEDI electron fluxes with pitch angles between 0 and 15° and with energies of ~25 to > 800 keV. (second panel) The Waves electric field spectral density for frequencies between 10^3 and 10^4 Hz. Similar upward trends are seen in both the JEDI and Waves data as well as matching times corresponding to peaks and valleys in the two data sets. (third panel) The JEDI electron fluxes plotted versus the integrated electric field spectral density from Waves (integrated over $10^3 - 10^4$ Hz). A high correlation corresponds to a positively sloped linear fit. The correlation coefficient (*R*) was calculated for the two data sets and found to be about 0.59.

incoherent and coherent processes, the latter relating to a plasma instability. Many early studies were based on the incoherent generation of whistler mode auroral hiss via Cerenkov radiation [*Ellis*, 1959; *Liemohn*, 1965; *Jorgensen*, 1968]. Cerenkov radiation occurs when the particles within a plasma move faster than the phase velocity of the wave. This can occur if the index of refraction is greater than one, such as near the resonance cone. This incoherent process was later dismissed by *Taylor and Shawhan* [1974] because of its inability to explain the amplitude of the observed emissions. Later, the idea of a coherent beam-to-plasma interaction near the Landau resonance velocity was proposed by *Maggs* [1976]. The coherent generation mechanism was also experimentally tested for its accuracy by a later study on the Spacelab 2 electron beam experiment [*Farrell et al.*, 1988]. This study found that the measured wave powers were greater than were expected from incoherent Cerenkov radiation and therefore must be generated by a coherent plasma instability. Hence, coherent plasma instabilities are currently the assumed local generation mechanisms for whistler mode emissions. Therefore, we conclude that our observed whistler mode wave emission is generated locally by an upgoing electron beam, ultimately caused by a coherent plasma instability.

4. Summary

This paper has investigated the characteristics of a new plasma wave emission observed over the high-latitude polar regions of Jupiter's magnetosphere. The emission observed on the Juno Waves instrument shows signatures in both the electric and magnetic fields, indicating that the wave is an electromagnetic wave. The spectrum's relation to the characteristic frequencies of the plasma shows that the electron cyclotron frequency is well above the frequency of the observed plasma wave emission for the entire duration of the pass. The emission also has one-half of a characteristic funnel-shape and shows similarities to whistler mode auroral hiss emissions previously observed near Earth. The plasma frequency was assumed to be ~20–40 kHz based on the conclusion that the emission is propagating in the whistler mode and frequency-dependent electric field spin modulation, similar to whistler mode auroral hiss studies from Earth. Another characteristic analyzed was the electric to magnetic field ratio. It was found that this ratio was approximately three near the start of the emission, then decreasing to about one for the remaining duration of the pass. It has been shown that the whistler mode can demonstrate characteristics similar to a nearly isotropic free-space mode when the cyclotron frequency is very high. However, at large wave normal angles, such as near the resonance cone, the E/cB ratio can become much greater than one.

The possible origins of this whistler mode emission were analyzed by performing a cross-correlation test between the flux of upgoing electron beams, observed by JEDI, and the integrated Waves electric field spectral density. A significant correlation was found with a correlation coefficient of 0.59. It is believed that the observed plasma wave emission is propagating in the whistler mode due to a plasma instability driven by a beam of upgoing electrons.

Acknowledgments
The authors would like to thank NASA and the various institutions that helped make the Juno mission possible. The research at the University of Iowa was supported by NASA through contract 699041X with Southwest Research Institute. The Juno data included herein will eventually be available from NASA's Planetary Data System. In the meantime, data may be requested from the lead author.

References

Connerney, J. E. P., M. H. Acuña, N. F. Ness, and T. Satoh (1998), New models of Jupiter's magnetic field constrained by the Io flux tube footprint, *J. Geophys. Res.*, *103*(A6), 11, 929–11, 939, doi:10.1029/97JA03726.

Connerney, J. E. P., et al. (2017), The Juno magnetic field investigation, *Space Sci. Rev.*, doi:10.1007/s11214-017-0334-z.

Ellis, G. R. A. (1959), Low-frequency electromagnetic radiation associated with magnetic disturbances, *Planet. Space Sci.*, *1*, 253–254, doi:10.1016/0032-0633(59)90029-7.

Farrell, W. M., D. A. Gurnett, P. M. Banks, R. I. Bush, and W. J. Raitt (1988), An analysis of whistler mode radiation from the Spacelab 2 electron beam, *J. Geophys. Res.*, *93*(A1), 153–161, doi:10.1029/JA093iA01p00153.

Gurnett, D. A. (1966), A satellite study of VLF hiss, *J. Geophys. Res.*, *71*(23), 5599–5615, doi:10.1029/JZ071i023p05599.

Gurnett, D. A., and A. Bhattacharjee (2005), *Introduction to Plasma Physics With Space and Laboratory Applications*, Cambridge Univ. Press, Cambridge, U. K.

Gurnett, D. A., S. D. Shawhan, and R. R. Shaw (1983), Auroral hiss, Z mode radiation, and auroral kilometric radiation in the polar magnetosphere: DE 1 observations, *J. Geophys. Res.*, *88*(A1), 329–340, doi:10.1029/JA088iA01p00329.

Gurnett, D. A., W. S. Kurth, J. T. Steinberg, P. M. Banks, R. I. Bush, and W. J. Raitt (1986), Whistler-mode radiation from the Spacelab 2 electron beam, *Geophys. Res. Lett.*, *13*(3), 225–228, doi:10.1029/GL013i003p00225.

James, H. G. (1976), VLF saucers, *J. Geophys. Res.*, *81*, 501–514, doi:10.1029/JA081i004p00501.

Jorgensen, T. S. (1968), Interpretation of auroral hiss measured on OGO-2 and at Byrd Station in terms of incoherent Cherenkov radiation, *J. Geophys. Res.*, *73*(3), 1055–1069, doi:10.1029/JA073i003p01055.

Liemohn, H. B. (1965), Radiation from electrons in magnetoplasma, *Radio Sci. J. Res. NBS/USNC-URSI*, *69D*(5), 741–765, doi:10.6028/jres.069D.084.

Maggs, J. E. (1976), Coherent generation of VLF hiss, *J. Geophys. Res.*, *80*(10), 1707–1724, doi:10.1029/JA081i010p01707.

Mauk, B. H., et al. (2013), The Jupiter Energetic Particle Detector Instrument (JEDI) investigation for the Juno mission, *Space Sci. Rev.*, 1–58, doi:10.1007/s11214-013-0025-3.

Mauk, B. H., et al. (2017), Juno observations of energetic charged particles over Jupiter's polar regions: Analysis of mono- and bi-directional electron beams, *Geophys. Res. Lett.*, *44*, doi:10.1002/2016GL072286.
Mitchell, D. G., et al. (2005), Energetic ion acceleration in Saturn's magnetotail: Substorms at Saturn?, *Geophys. Res. Lett.*, *32*, L20S01, doi:10.1029/2005GL022647.
Mosier, S. R., and D. A. Gurnett (1969), VLF measurements of the Poynting flux along the geomagnetic field with the Injun 5 satellite, *J. Geophys. Res.*, *74*(24), 5675–5687, doi:10.1029/JA074i024p05675.
Santolik, O., and D. A. Gurnett (2002), Propagation of auroral hiss at high altitudes, *Geophys. Res. Lett.*, *29*(10), 1481, doi:10.1029/2001GL013666.
Smith, R. L. (1969), VLF observations of auroral beams as sources of a class of emissions, *Nature*, *224*(5217), 351–352, doi:10.1038/224351a0.
Stix, T. H. (1962), *The Theory of Plasma Waves*, McGraw-Hill, New York.
Taylor, W. W. L., and S. D. Shawhan (1974), A test of incoherent Cerenkov radiation for VLF hiss and other magnetospheric emissions, *J. Geophys. Res.*, *79*(1), 105–117, doi:10.1029/JA079i001p00105.